Purified Native Microtubule Associated Protein MAP1A: Kinetics of Microtubule Assembly and MAP1A/Tubulin Stoichiometry†

Barbara Pedrotti‡ and Khalid Islam*,§

Department of Biology, University of Milan, Via Celoria 26, Milano, Italy, and Lepetit Research Center, Marion Merrell Dow Research Institute, Via R. Lepetit 34, Gerenzano (Va), Italy

Received January 20, 1994; Revised Manuscript Received July 28, 1994®

ABSTRACT: In a recent study, we have shown that sulfonate buffers affect microtubule assembly and alter microtubule protein composition (Pedrotti et al., 1993). In particular, we noted that PIPES buffer leads to removal of MAP1 from the microtubule surface without affecting the association of MAP2 with microtubules. This observation has been exploited to develop a simple purification procedure for MAP1A using twice-cycled microtubule protein prepared from whole bovine brain. A single chromatographic step on an ion-exchange column results in >90% pure MAP1A. Using purified MAP1A, we now show that MAP1A (a) binds in a dose-dependent manner to unpolymerized tubulin and assembled microtubules, (b) binds 13–15 mol of tubulin dimers in assembled microtubules, (c) promotes both nucleation and elongation of tubulin, and (d) promotes incorporation of tubulin dimers at low GTP concentrations and of tubulin dimers and oligomers at high GTP concentrations. MAP1A lowers the critical concentration for assembly, and MAP1A-promoted incorporation of dimers has an association rate constant (K_{+1}) of 39.3×10^6 $M^{-1}s^{-1}$ and a dissociation rate constant (K_{-1}) of 15 s^{-1}; both constants are about 2–3-fold higher compared with MAP2.

Microtubule protein purified by temperature-dependent cycles of polymerization and depolymerization from brain sources consists of tubulin and microtubule associated proteins (MAPs)[1] [for reviews, see Olmsted (1986), Wiche (1989), Matus (1990), and Tucker (1990)]. MAPs, e.g., MAP2 and tau, have been shown to promote microtubule assembly *in vitro* and affect the dynamic instability and treadmilling behavior of microtubules (Johnson & Borisy, 1977; Cleveland et al., 1977; Burns & Islam, 1986; Wilson & Farrell, 1986; Farrell et al., 1987; Wiche, 1989). High molecular mass MAPs, namely, MAP1 (about 350 kDa) and MAP2 (200 kDa), have been reported to form long thin projections from microtubule surfaces implicated in microtubule bundling and cross-linking microtubules with other cytoskeletal components (Chen et al., 1992). The important role played by MAPs in regulating cellular processes is further highlighted by the observations that MAPs exhibit aberrant modifications and/or distribution in a number of neurodegenerative disorders (Hasegawa et al., 1990; Mandelkow & Mandelkow, 1993).

High molecular mass MAP1 and MAP2 are composed of multiple species termed MAP1A, MAP1B, MAP1C, MAP2A, and MAP2B from the slowest to the fastest migrating species on SDS–PAGE (Bloom et al., 1984b). While MAP2A and MAP2B are closely related polypeptides encoded by a single gene, MAP1A, MAP1B, and MAP1C are encoded by three distinct genes (see below). MAP1C has been identified as a cytoplasmic dynein involved in retrograde motion (Paschal & Vallee, 1987), but the functions of MAP1A and MAP1B are essentially unknown.

MAP1A and MAP1B are more widely distributed compared with the essentially dendritic localization of MAP2A and MAP2B (Matus, 1988), being found in both dendrites and axons of neurons as well as in glial cells. MAP1A has also been reported to be present in interphase and mitotic microtubules in various tissue culture cells, suggesting more general functions (Bloom et al. 1984a). MAP1B is especially prominent in axons during initial outgrowth, suggesting a role in neurogenesis and process plasticity, while MAP1A is expressed at later stages (Matus, 1988).

The complete nucleotide sequences for MAP2 (Lewis et al., 1988), MAP1A (Langkopf et al., 1992), and MAP1B (Noble et al., 1989) have been determined. The C-terminal region of MAP2 contains 3, 18 amino acid basic imperfect repeats which constitute the microtubule binding site (Lewis et al., 1988). Positively charged repeat motifs have also been identified in MAP1A and MAP1B. These motifs, which may constitute the microtubule binding site, are similar in both proteins (Langkopf et al., 1992; Noble et al., 1989), but are different from those present in MAP2. However, despite the sequence similarities between MAP1A and MAP1B, the two proteins exhibit different binding affinity to microtubules during cycles of polymerization: MAP1A associates and pellets with assembled microtubules while MAP1B remains in the supernatant (Bloom et al., 1985; Pedrotti et al., 1993). At a structural level, the thin filamentous shape of the MAP1A molecule closely resembles that of MAP2, and both proteins have been colocalized to the same microtubules in vivo (Shiomura & Hirokawa, 1987) and in vitro (Chen et al., 1992; Pedrotti et al., 1993).

Most biochemical studies on high molecular weight MAPs have used purified MAP2, consisting of both MAP2A and MAP2B polypeptides, to characterize interaction with tubulin,

† This work was supported by an Italian Ministry of Science and Technology student grant to B.P.

* Author to whom correspondence should be addressed. Telephone: 02 96474453/96474380. Fax: 02-96474365.

‡ University of Milan.

§ Marion Merrell Dow Research Institute.

® Abstract published in *Advance ACS Abstracts,* September 1, 1994.

[1] Abbreviations: EGTA, ethylene glycol bis(β-aminoethyl ether)-*N,N,N′,N′*-tetraacetic acid; EDTA, ethylenediaminetetraacetic acid; GTP, guanosine 5′-triphosphate; MAP(s), microtubule-associated protein(s); MES, 2-(*N*-morpholino)ethanesulfonic acid; PIPES, piperazine-*N,N′*-bis(2-ethanesulfonic acid); SDS, sodium dodecyl sulfate; PAGE, polyacrylamide gel electrophoresis; PBS, phosphate-buffered saline; Tris, Trizma base; PMSF, phenylmethanesulfonyl fluoride; DTT, DL-dithiothreitol.

0006-2960/94/0433-12463$04.50/0

microtubules, and other cytoskeletal components (Leterrier et al., 1982; Suprenant & Dentler, 1982; Satillaro, 1986; Pedrotti et al., 1994a). Similar studies with native purified MAP1A or MAP1B proteins are lacking as there are no satisfactory purification procedures. Attempts to purify MAP1 from brain white matter, to avoid contamination by MAP2 by taking advantage of its spatial location in brain tissue, have resulted in low yields of protein (Vallee, 1982). Bulk separation of MAP1 from MAP2 components revealed that MAP1A and/or MAP1B is/are capable of promoting assembly (Kuznetsov et al., 1981; Vallee, 1982; Vera et al., 1988).

We have recently shown that MAP1A promotes microtubule assembly by examining the effect of sulfonate buffers (Pedrotti et al., 1993). We now describe a procedure which uses twice-cycled microtubule protein prepared from whole bovine brain for the purification of MAP1A. Experiments using purified native MAP1A demonstrate that it is capable of promoting assembly. The purification protocol, the interaction with microtubules and tubulin, the stoichiometry of MAP1A/tubulin in assembled microtubules, and the kinetics of tubulin polymerization are described.

EXPERIMENTAL PROCEDURES

The following buffers were used: MES buffer (0.1 M MES, 2.5 mM EGTA, 0.5 mM $MgCl_2$, 0.1 mM EDTA, and 1 mM DTT, pH 6.4, with KOH); PIPES buffer (0.1 M PIPES, 2.5 mM EGTA, 0.5 mM, $MgCl_2$, 0.1 mM EDTA, and 1 mM DTT, pH 6.9, with KOH).

Purification of Microtubule Protein. Bovine brain microtubule protein was prepared by two cycles of temperature-dependent assembly/disassembly according to Islam and Burns (1981) as modified by Pedrotti et al. (1993). Briefly, whole brain was homogenized in PIPES buffer, containing 0.1 mM PMSF and 40 μg/mL leupeptin, and after centrifugation, the supernatant was adjusted to 20% glycerol and 1 mM GTP and incubated at 37 °C for 20 min. At the end of the incubation period, the assembled protein was collected by centrifugation, and the pellets were resuspended in MES buffer and cold-dissociated at 4 °C for 60 min. After removal of the cold-stable material by centrifugation, the supernatant was adjusted to 1 mM GTP, in the absence of glycerol, and all other steps were performed in MES buffer as described previously (Islam & Burns, 1981). Microtubule protein (15–20 mg/mL) was frozen and stored in liquid nitrogen.

We use this rather unusual protocol as PIPES buffer compared with MES buffer results in a better extraction of proteins from brain (5440 vs 4100 mg, respectively) and a higher yield of assembled protein (1351 vs 1120 mg, respectively). However, further purification in PIPES buffer resulted in a decrease in the recovery of microtubule protein (5.9% vs 7.2% in PIPES vs MES buffer, respectively). More importantly, a loss of the MAP1 protein was observed when the second cycle of assembly was performed in PIPES buffer. By contrast, MAP1 remained associated with microtubules when assembly was performed in MES buffer (Pedrotti et al., 1993; unpublished observation). The buffer conditions used in the purification protocol have been specifically selected to increase the total amount both of microtubule protein (ca. 1 mg/g of brain tissue) and of MAP1A.

Purification of Tubulin and MAPs. Tubulin was purified from twice-cycled microtubule protein by column chromatography using a Mono-Q resin (HR 5/5, Pharmacia) on the Pharmacia FPLC system. The column was equilibrated in MES buffer, containing 50 μM GTP and 0.1 mM PMSF, and 20–30 mg of twice-cycled protein was loaded onto the column and subsequently washed with 15 column volumes of the equilibration buffer. The associated proteins were eluted with the same buffer containing 0.4 M NaCl and bound tubulin by raising the NaCl concentration to 1 M. Tubulin and MAPs were dialyzed for 2 h vs 100 volumes of equilibration buffer and used immediately for the assembly studies. Gel exclusion chromatography on a Superose 12 column showed that the dialyzed tubulin was dimeric (mass = 110 000 kDa) and no tubulin oligomers were present; no protein was observed in the void fractions.

Heat-treated MAP2 was prepared according to Herzog and Weber (1978) and purified by FPLC. Native MAP1A was purified as described in the text (see Results).

Tubulin Binding and Polymerization. Tubulin polymerization was performed as described previously (Pedrotti et al., 1993). Taxol-stabilized microtubules were prepared by polymerization in MES buffer containing 250 μM GTP and 10 μM taxol. For the binding studies, the taxol-stabilized microtubules were layered on top of a 30% sucrose cushion and centrifuged at 150000*g* for 25 min at 37 °C in a TL-100 Beckman ultracentrifuge (Pedrotti et al., 1993).

Solid-phase immunoassay to determine binding to unpolymerized and polymerized tubulin was performed on 96-well microtiter plates as described previously (Pedrotti et al., 1994a). Briefly, microtiter wells were coated with the substrate proteins by incubating either 0.1 mg/mL taxol-stabilized microtubules or tubulin for 2 h; the solution was then removed, and remaining protein sites were blocked using 5% glycine for 2 h. After blocking, the wells were challenged with increasing concentrations of MAP1A, and, after washing any unbound MAP1A, the substrate-bound MAP1A was detected using the anti-MAP1A monoclonal antibody. A secondary anti-IgG antibody labeled with horseradish peroxidase was used to recognize the primary antibody, and color development in the presence of the peroxidase substrate was determined at 492 nm.

Control wells were identically treated except that either the substrate coating step or alternatively the MAP challenge step was omitted.

Determination of Seed Concentration. Aliquots of microtubules assembled to steady state were fixed by dilution in 0.1% glutaraldehyde and negatively stained (Islam & Burns, 1984). Microtubule lengths were measured from electron micrographs (100–150 microtubules), and the number concentration was calculated from the amount of polymerized protein and the mean microtubule length (Pedrotti et al., 1993).

Protein Composition and Western Blotting. Proteins were fractionated by denaturing SDS–PAGE using the Pharmacia Phast system. The gels were stained and the integrated peak areas determined as described previously (Pedrotti et al., 1993). For dot blots, 2 μL of protein solution was directly spotted onto nitrocelloluse membranes while for Western blots the proteins were fractionated by SDS–PAGE and transferred onto nitrocellulose membranes (Towbin & Gordon, 1984) and immunostained using MAP2, MAP1A, MAP1B (Amersham), and tau-2 (Sigma Chemical Co.) monoclonal antibodies.

Determination of Protein Content. Protein concentration was determined using the Bradford method (Bio-Rad protein reagent kit), and bovine serum albumin was used as a standard.

RESULTS

MAP1 has been reported to be either thermolabile (Kuznetsov et al., 1981) or thermostable (Vera et al., 1988). We

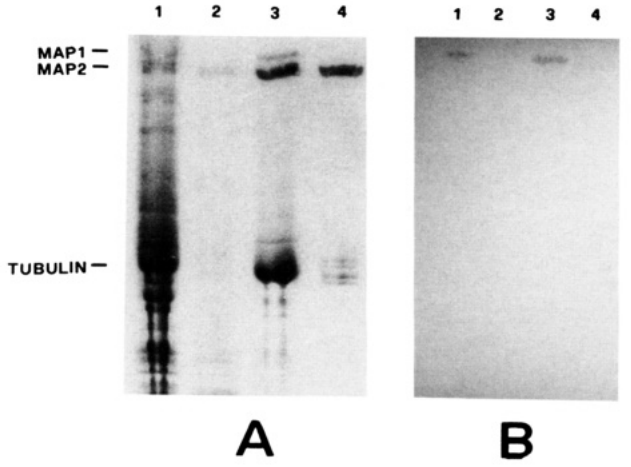

FIGURE 1: Effect of thermal treatment on MAP1 and MAP2 in whole brain supernates and twice-cycled microtubule protein. Thermal treatment of whole brain supernates or twice-cycled microtubule protein, 100 °C for 5 min, was carried out essentially as described by Vera et al. (1988). The protein was fractionated by SDS–PAGE on 4–15% acrylamide gradient gels and either (A) stained with Coomassie brilliant blue R-250 or (B) transferred onto nitrocellulose filters and immunostained with the anti-MAP1A antibody. Lanes: whole brain supernate before (1) and after (2) thermal treatment; twice-cycled microtubule protein before (3) and after (4) thermal treatment.

examined the effect of heat treatment (100 °C for 5 min) on MAP1 using either whole brain supernates or twice-cycled microtubule protein. After the thermal step, the precipitated protein was removed by centrifugation, and the supernatants were analyzed by SDS–PAGE. Under these conditions, little or no MAP1 was observed in the heat-treated supernatants although significant amounts of MAP2 were present (Figure 1A). Western blotting using the anti-MAP1A monoclonal antibody confirmed the absence of MAP1A in the heat-treated samples (Figure 1B).

In our preparations, twice-cycled microtubule protein typically consists of 60% tubulin, 13% MAP2, and 11% MAP1, the remainder being minor contaminants (Figure 1; Pedrotti et al., 1993). MAP1A was the major MAP1 polypeptide in such preparations; MAP1B is largely lost in the first cycle (Pedrotti et al., 1993). Assembly of such protein in PIPES buffer results in the loss of MAP1 from the microtubule surface (Pedrotti et al., 1993), and we exploited this observation to develop the procedure described below.

Purification of MAP1 Protein. Step 1. Twice-cycled microtubule protein was assembled in MES buffer in the presence of taxol, and the assembled microtubules were collected by centrifugation (100000*g*, 25 min, 37 °C). The supernatant was discarded, and the pellets were gently resuspended in the starting volume of warm PIPES buffer containing 20 μM taxol and incubated for a further 20 min at 37 °C, to allow reassembly of disrupted microtubules, prior to centrifugation (100000*g*, 25 min, 37 °C). The proteins in the pellet and the supernatant when analyzed by SDS–PAGE showed that MAP1 was present in the supernatant, with some tubulin and minor protein components, and only trace amounts of MAP1A remain associated with the pellet (Figure 2, cf. lanes 2 and 3). To ensure complete removal of MAP1, the polymerized protein was resuspended in warm PIPES buffer and taken through a further cycle. The two supernatants were then pooled and used for the next step. All further steps were performed at 4–8 °C unless otherwise stated.

Step 2. The pooled supernatant was loaded onto a Mono-Q column (HR 10/10, Pharmacia), and subsequently the column

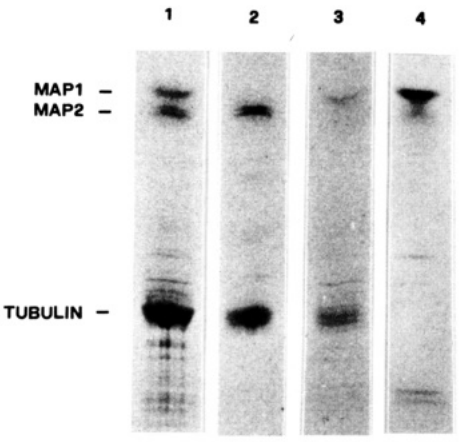

FIGURE 2: SDS–PAGE analysis of the MAP1 purification steps. The protein at different stages of purification was fractionated by SDS–PAGE on 4–15% acrylamide gradient gels and stained with Coomassie brilliant blue R-250. Lanes: (1) twice-cycled microtubule protein; (2) PIPES pellet; (3) PIPES supernatant; and (4) FPLC-purified MAP1.

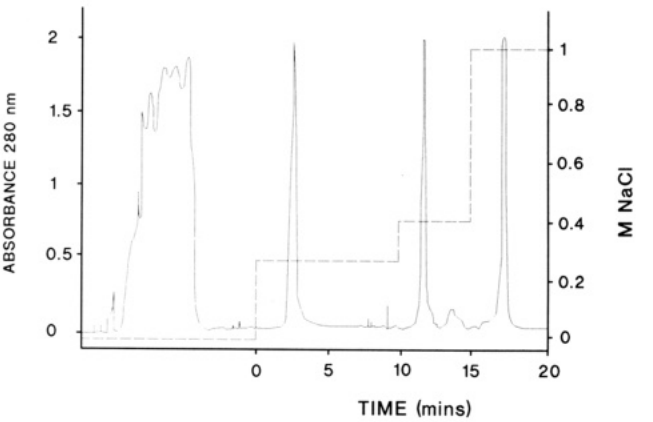

FIGURE 3: FPLC profile of elution from the Mono Q resin. 73 mg of PIPES supernatant protein (see Results and Figure 2) was loaded onto a Mono-Q column (HR 10/10, Pharmacia), preequilibrated in MES buffer, at a flow rate of 1 mL/min. The unbound protein was removed by washing the column with the equilibration buffer, until the absorbance at 280 nm was close to zero, and the bound protein eluted at a flow rate of 4 mL/min with the indicated salt steps. MAP1 protein eluted in 0.4 M NaCl (see Figure 2).

was washed with 20 volumes of MES buffer, containing 0.1 mM PMSF, until no further protein eluted. The bound protein was eluted from the column using several salt steps (Figure 3), and SDS–PAGE analysis showed that MAP1 eluted in the 0.4 M NaCl step (Figure 2). Tubulin eluted in the 1 M NaCl step and most of the minor components in the 0.25 M NaCl step.

Using this procedure, we typically obtain about 16 mg of purified MAP1 from about 300 g of brain tissue (300–350 mg of twice-cycled protein). The purified MAP1 protein after desalting, by dialysis against 100 volumes of MES buffer, can be stored at −80 °C for over 6 months without loss of activity.

Characterization of MAP1 Protein. The FPLC-purified MAP1 protein, eluted in the 0.4 M NaCl step, was analyzed by SDS–PAGE and by blotting after transfer onto nitrocellulose membranes. Immunostaining of dot blots using commercially available monoclonal antibodies (see Experimental Procedures) with well-characterized specificities—anti-MAP1A-1 (Bloom et al., 1984a,b), anti-MAP1B-4 (Bloom et al., 1985), anti-MAP2.3 (Cambray-Deakin et al., 1987), and anti-tau-2 (Papasozomenos & Binder, 1987)—showed

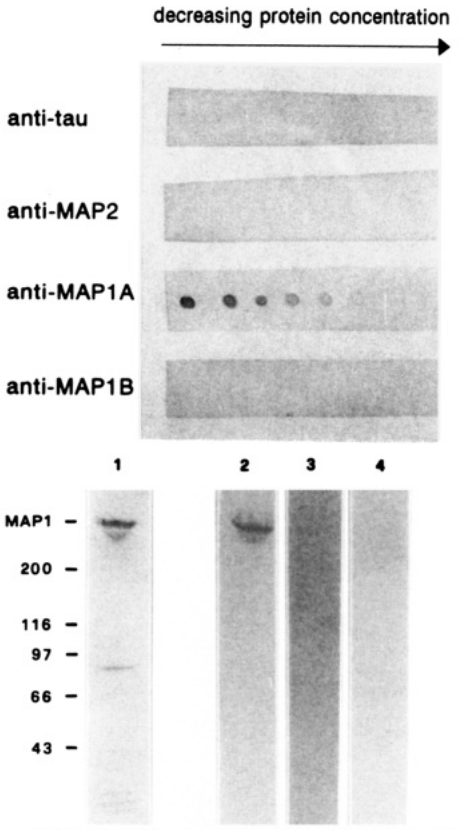

FIGURE 4: SDS–PAGE and Western blotting of purified MAP1 with monospecific monoclonal antibodies. (A) Six serial (1:2) dilutions of FPLC-purified MAP1 protein were spotted onto nitrocellulose membranes and immunostained using the indicated anti-MAP antibodies. The protein was specifically recognized by the anti-MAP1A antibody but not by the anti-tau, anti-MAP2, or anti-MAP1B monoclonal antibodies. (B) MAP1 protein was fractionated by SDS–PAGE on 4–15% acrylamide gradient gels under denaturating conditions and either stained with Coomassie brilliant-blue (lane 1) or blotted and immunostained using the anti-MAP1A (lane 2), anti-MAP1B (lane 3), or anti-MAP2 (lane 4) monoclonal antibodies. Molecular mass standards are indicated in kilodaltons.

that the protein was stained only by the MAP1A antibody but not by the MAP2, tau, or MAP1B antibodies (Figure 4A).

SDS–PAGE analysis (Figure 4B, lane 1) showed that the protein consisted of several bands with apparent molecular masses of about 350, 280, 70, 30, 28, and 17 kDa. Western blotting showed that the two high molecular mass (350 and 280 kDa) bands were intensely stained by the MAP1A antibody with little or no detectable staining observed with MAP2 or MAP1B antibodies (Figure 4B). The 280 kDa band therefore represents a proteolytic degradation product of the high molecular mass MAP1A protein.

Densitometric scanning of Coomassie-stained gels (Figure 5) and calculation of the integrated peak areas showed that the two high molecular mass MAP1A bands, the heavy chain, comprised about 75% of the total protein. The low molecular mass bands of 30, 28, and 17 kDa constituted about 8%, 7%, and 4% of the total protein and probably represent the tightly associated light chains (LC1, LC2, and LC3) of MAP1A (Kuznetsov et al., 1986; Langkopf et al., 1992; Schoenfeld et al., 1989). The estimated molar abundance of each light chain with respect to the heavy chain was typically about 1 mol/mol. The 70 kDa band [the identity of this protein is not known, but it has also been observed in MAP1A obtained by immunoprecipitation (Schoenfeld et al., 1989)] represented about 5–6% of the total protein.

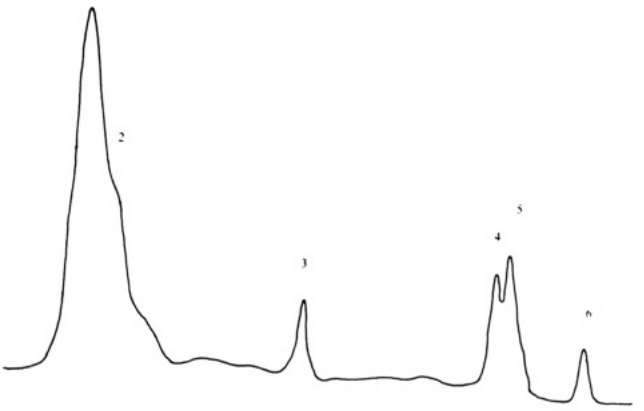

FIGURE 5: Densitometric scan of purified MAP1A protein. Purified MAP1A was fractionated by SDS–PAGE on 4–15% acrylamide gradient gels under denaturing conditions and stained with Coomassie brilliant-blue. The stained gels were densitometrically scanned on an LKB densitometer equipped with a peak integrator. The apparent molecular masses of the indicated peaks are (1) 350, (2) 280, (3) 70, (4) 30, (5) 28, and (6) 17 kDa.

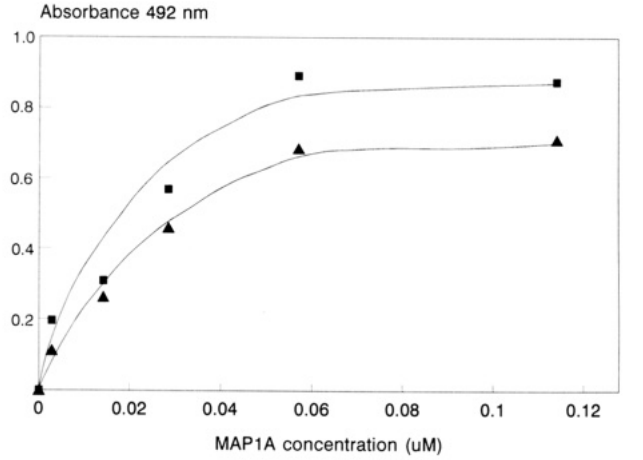

FIGURE 6: Solid-phase immunoassay for MAP1A binding to tubulin and microtubules. Taxol-stabilized microtubules (0.1 mg/mL; ■) or FPLC-purified tubulin (0.1 mg/mL; ▲) was coated onto microtiter wells (see Experimental Procedures) and, after blocking of remaining protein sites with 5% glycine, challenged with the indicated concentrations of purified MAP1A. The substrate-bound MAP1A was detected using the anti-MAP1A monoclonal antibody. A secondary antibody labeled with horseradish peroxidase was used to detect the primary antibody, and after addition of the peroxidase substrate, the absorbance at 492 nm was determined using the Titertek Multiscan MCC/340 microtiter plate reader.

Binding of Purified MAP1A to Unpolymerized and Polymerized Tubulin. We used a solid-phase immunoassay (Pedrotti et al., 1994a) to determine the ability of MAP1A to interact with unpolymerized and polymerized tubulin. Microtiter wells coated with taxol-stabilized microtubules or unpolymerized tubulin were challenged with the indicated concentrations of MAP1A, and the substrate-bound MAP1A was revealed by color development at 492 nm (see Experimental Procedures). MAP1A binding increased as the MAP1A concentration was raised and tended to achieve a plateau at high concentrations (Figure 6), suggesting a concentration-dependent binding to the substrates. Maximal MAP1A binding to unpolymerized tubulin and polymerized microtubules was about 60 nM, although the amount of MAP1A that bound to tubulin was somewhat lower compared with microtubules.

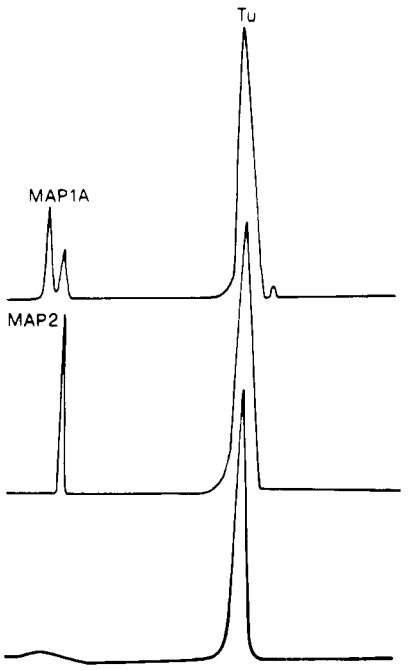

FIGURE 7: Densitometric scans of MAP1A and MAP2 copelleting with taxol-stabilized microtubules. Taxol-stabilized microtubules incubated either in the presence of the MAP1A and MAP2 or in the absence of MAPs were centrifuged through a sucrose cushion (see Results). After resuspension, the protein in the pellets was fractionated by SDS–PAGE, and, after staining and destaining, the gels were scanned at 595 nm using a LKB densitometer. The protein bands corresponding to purified MAP1A, MAP2, and tubulin are indicated, and the integrated peak areas of such scans were used to determine the MAP/tubulin stoichiometry (see Table 1).

Determination of MAP1A/Tubulin Stoichiometry of Assembled Microtubules. The MAP1A/tubulin stoichiometry in assembled microtubules was determined by sedimentation. Taxol-stabilized microtubules (tubulin 0.8 mg/mL) incubated in the presence of different concentrations of either MAP1A or MAP2 were centrifuged through a 30% sucrose cushion. Pellets were resuspended and fractionated by SDS–PAGE , and after being stained, the gels were scanned and integrated peak areas determined (Figure 7). Intact MAP1A (350 kDa), the high molecular mass (280 kDa) degradation product, and the light chains (30, 28, and 17 kDa) all cosedimented with assembled microtubules while the 70 kDa protein was found in the supernatant.

The stoichiometry was determined from the integrated peak areas corrected for the molecular mass of the proteins (350 and 280 kDa for MAP1A and the degradation product, respectively; 200 kDa for MAP2 and 100 kDa for tubulin); the Coomassie Blue stain binding/mass of protein has been assumed to be constant for all proteins (Burns & Islam, 1984; unpublished observation). Initially, as the MAP concentration was increased, the MAP/tubulin stoichiometry decreased but at higher concentrations remained essentially unaltered (Table 1), representing the final stoichiometry. The calculated MAP2/tubulin dimer stoichiometry was 1:(8–9) mol/mol, which is in close agreement with that reported previously (Amos, 1977; Burns & Islam, 1984; Wallis et al., 1993; the previously reported values have been corrected for the molecular mass of MAP2 calculated from the known sequence). The MAP1A/tubulin dimer stoichiometry was about 1:(13–15) mol/mol. A similar stoichiometry for both MAPs was also determined in twice-cycled microtubules where the MAP1A/tubulin and MAP2/tubulin stoichiometries were

Table 1: Determination of MAP1A/Tubulin Dimer or MAP2/Tubulin Dimer Stoichiometry[a]

MAP2 added[b] (mg/mL)	tubulin[c] (μg)	MAP2[c] (μg)	tubulin/MAP2 stoichiometry (mol/mol)
0.15	36.42	5.05	14.5
0.20	49.27	6.07	16.4
0.26	43.02	11.6	7.43
0.31	43.25	9.1	9.52
MAP1A added[b] (mg/mL)	**tubulin[c] (μg)**	**MAP1A[c] (μg)**	**tubulin/MAP1A stoichiometry (mol/mol)**
0.50	34.79	5.66	23.9
0.68	42.37	11.19	15.0
1.09	38.65	11.83	13.0

[a] Taxol-stabilized microtubules, composed of FPLC-purified tubulin, were incubated in the presence of different concentrations of MAP1A or MAP2. The assembled microtubules were pelleted through a sucrose cushion, and the proteins in the pellets were fractionated by SDS–PAGE and stained with Coomassie brilliant blue. The gels were scanned (see Figure 6) and the integrated peak areas for MAP1A, MAP2, or tubulin determined. The stoichiometry was calculated following correction for the molecular mass of the proteins: 200 kDa for MAP2, 100 kDa for tubulin, 350 and 280 kDa for MAP1A and the degradation product. [b] The initial concentration of MAP added to taxol-stabilized microtubules. [c] The amount of MAP and tubulin recovered in the pellets was determined from the integrated peak areas after scanning.

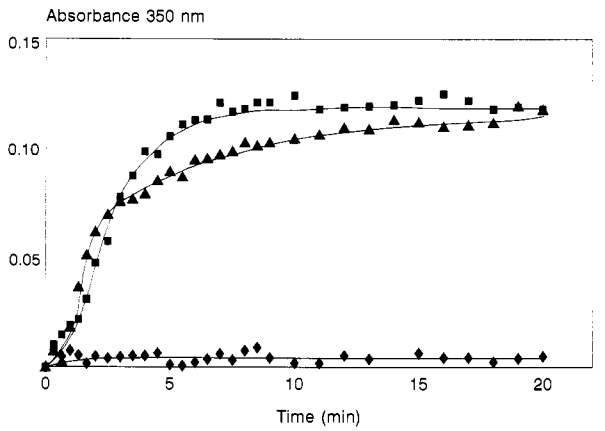

FIGURE 8: Polymerization of purified tubulin in the absence of MAPs or in presence of MAP1A or MAP2. FPLC-purified tubulin (1 mg/mL) in MES buffer, containing 500 μM GTP, was incubated at 30 °C either in the absence of MAPs (♦) or in the presence of 0.32 mg/mL MAP1A (▲) or 0.18 mg/mL MAP2 (■). The polymerization was monitored by the change in absorbance at 350 nm in a Shimadzu UV2100 spectrophotometer fitted with a temperature-controlled compartment.

1:19 and 1:10 mol/mol, respectively (see Figure 1; Pedrotti et al., 1993).

Effect of MAP1A on Tubulin Polymerization. Microtubule assembly conforms to a linear condensation polymerization reaction requiring nucleation and elongation events (Oosawa & Kasai, 1962). To determine if MAP1A could promote tubulin polymerization, purified tubulin was incubated either in the presence of MAP2 or MAP1A or in the absence of associated proteins. Under these conditions, pure tubulin was not capable of polymerization (Figure 8) but polymerized in the presence of either MAP2 or MAP1A. Typical microtubule assembly was observed with an initial lag phase, representing the nucleation events, followed by elongation and the achievement of a more or less stable plateau by about 10–15 min. The final extent of polymerization was similar for both MAP1A and MAP2 (Figure 8), and this was confirmed by pelleting the polymerized protein. Electron microscopy revealed the presence of negatively stained microtubules in samples

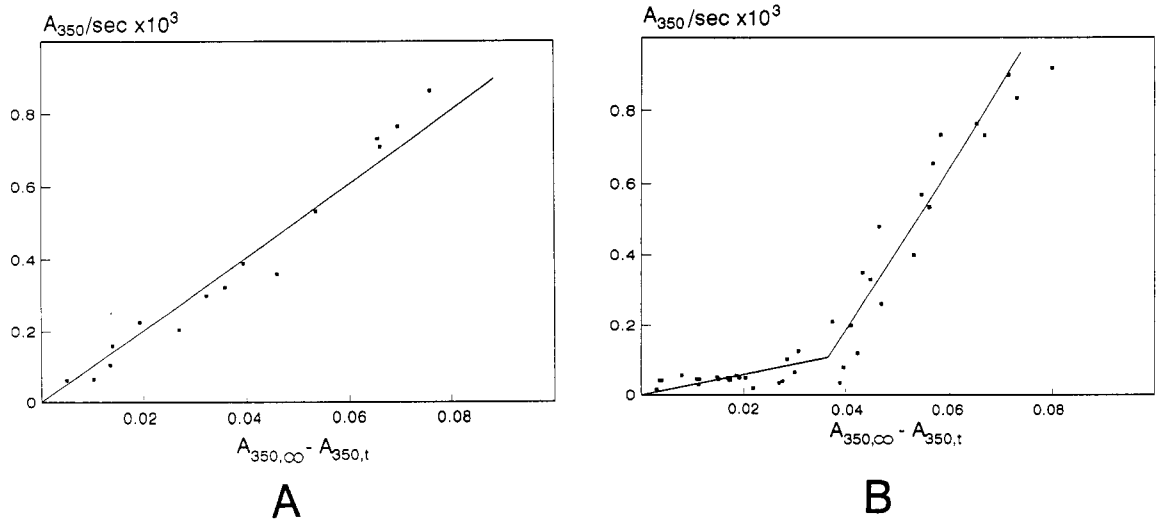

FIGURE 9: Pseudo-first-order plots of MAP1A- or MAP2-promoted assembly at a high (500 μM) GTP concentration. The rate of MAP2-promoted (A) and MAP1A-promoted (B) tubulin polymerization (A_{350}/s) is plotted against the instantaneous free subunit concentration ($A_{350nm,\infty} - A_{350nm,t}$). Data from the nucleation phase have been omitted, and representative points are presented as the assembly approaches equilibrium. The absorbance increase as a function of time for MAP1A- and MAP2-promoted assembly is shown in Figure 8.

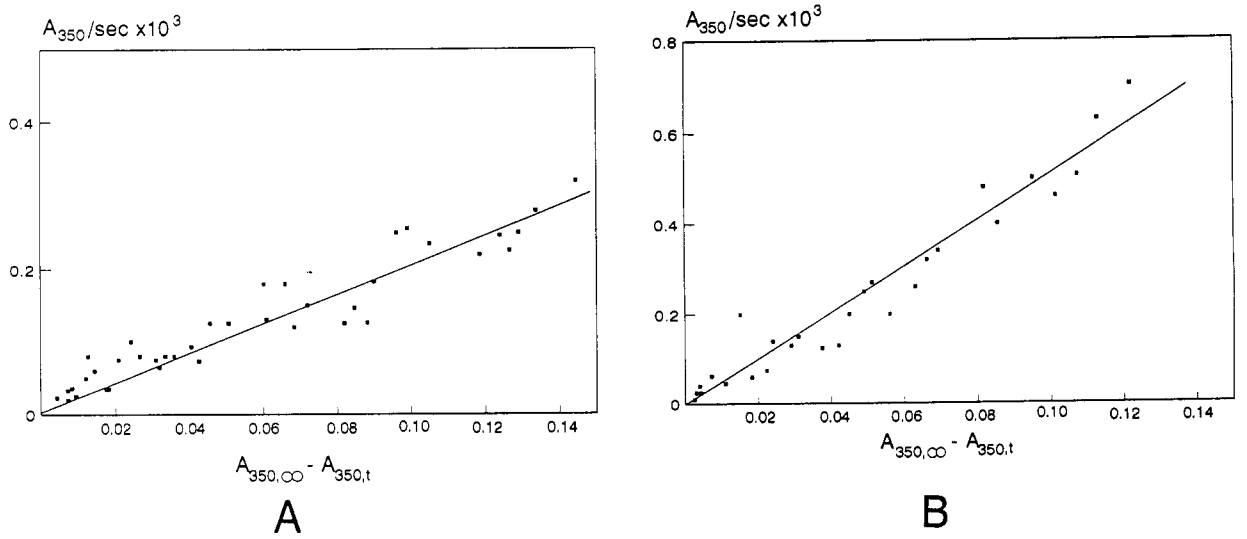

FIGURE 10: Pseudo-first-order plots of MAP1A- and MAP2-promoted assembly at a low (40 μM) GTP concentration. FPLC-purified tubulin was polymerized in MES buffer containing 40 μM GTP in the presence of either MAP2 (A) or MAP1A (B). The rate of tubulin polymerization (A_{350}/s) is plotted against $A_{350nm,\infty} - A_{350nm,t}$ as in Figure 9.

containing MAP1A or MAP2; no microtubules were observed in the pure tubulin sample (not shown).

Kinetics of Microtubule Assembly. In the presence of MAPs, tubulin exists as a mixture of dimers and oligomers, and while both species can be directly incorporated into microtubules at high GTP concentrations, mainly dimers are incorporated at low GTP concentrations (Islam & Burns, 1986; Burns, 1991). MAP1A- and MAP2-promoted microtubule assembly at high GTP concentration (see figure 8) was examined using pseudo-first-order plots (Islam & Burns, 1986). Upon completion of the nucleation phase, MAP2-promoted assembly was described by a single reaction (Figure 9A) with an apparent rate of 10.4×10^{-3} s^{-1}. By contrast, MAP1A-promoted assembly was described by the summation of two reactions (Figure 9B): in the early stages of elongation with an apparent rate of 24.3×10^{-3} s^{-1} and in later stages with an apparent rate of 2.85×10^{-3} s^{-1}. While the differences in the apparent rate between MAP2 and MAP1A may reflect the number of nucleation sites, the biphasic kinetics are most likely due to the different rates of incorporation of dimers and oligomers into the growing microtubules.

In a separate experiment, we also examined the kinetics at a low (40 μM) GTP concentration. At the low GTP concentration, a single reaction was observed for both MAP1A- and MAP2-promoted polymerization with apparent rates of 5.1×10^{-3} and 2.2×10^{-3} s^{-1}, respectively (Figure 10). The apparent reaction rate and the number concentration of the nucleation sites (see Experimental Procedures) were used to calculate the association rate constants: K_{+1} for MAP1A-promoted polymerization was 39.3×10^6 M^{-1} s^{-1} and for MAP2-promoted polymerization was 19.8×10^6 M^{-1} s^{-1}.

The steady-state critical concentration for MAP1A- and MAP2-assembled microtubules, determined by diluting pre-assembled microtubules to various protein concentrations, was 0.35 and 0.24 μM, respectively. The critical concentration for microtubule assembly at steady-state, for MAP-rich microtubules exhibiting minimal dynamic instability (Farrell et al., 1987; Horio & Hotani, 1986), represents the sum of the net dissociation rate over the net association rate. The

sum of the critical concentration and the association rate constant yields a dissociation rate constant of 14 and 4.8 s^{-1} for MAP1A- and MAP2-promoted polymerization, respectively.

DISCUSSION

Microtubule associated proteins (MAPs) have been demonstrated to affect microtubule assembly dynamics, implying an important role for MAPs in the structural organization of the cytomatrix. Their differential distribution, regulated spatially and temporally, in neuronal and nonneuronal cells has suggested that these proteins may give rise to different subsets of microtubules. More recently, alteration in MAP expression or structure has been implicated in several neurodegenerative disorders (see the introduction).

Of the different high molecular mass MAPs, only MAP2, consisting of both MAP2A and MAP2B isoforms, has been studied in some detail as MAP2 is heat-stable and can be easily purified using a thermal step (Herzog & Weber, 1978). MAP1 has been reported to be both heat-labile (Kuznetsov et al., 1981) and heat-stable (Vera et al., 1989). We find that MAP1A in whole brain supernates or twice-cycled microtubule protein is heat-labile (Figure 1), although purified MAP1A is thermostable (data not shown). Vallee (1985) has also shown that MAP1, consisting mainly of MAP1A, is thermolabile in the presence of tubulin or BSA but becomes heat-stable when freed of other proteins. The lability or stability of MAP1A to heat treatment therefore depends on other factors rather than being a property of the protein itself. Variations in the source, isolation conditions, buffer conditions, or composition of protein may be responsible for the observed lability (Figure 1; Kuznetsov et al., 1981; Vallee, 1993) or stability (Vera et al., 1988) of MAP1A in whole brain supernates. Alternatively, since the MAP1 composition in the earlier reports (Kuznetsov et al., 1981; Vera et al., 1988) was not examined, it is at least possible that MAP1A was the major MAP1 species in the preparations of Kuznetsov et al. (1981) while MAP1B may have been the predominant MAP1 species in those of Vera et al. (1988).

Earlier studies using bulk MAP1 have shown that it is able to promote microtubule assembly. In a recent study, we have provided the first evidence that MAP1A promotes microtubule assembly (Pedrotti et al., 1993). On the basis of our previous results, we have developed a simple purification procedure for MAP1A which results in high yields of purified protein. Our procedure has several important advantages over those described previously by Kuznetsov et al. (1981) and Vallee (1982): (1) Twice-cycled microtubule protein prepared from whole brain protein can be used, avoiding the need for dissecting white matter; (2) a single MAP1 species, namely, MAP1A, is purified with little or no contamination from MAP2, MAP1B, or tau; (3) the procedure is relatively simple; (4) high yields of MAP1A are obtained. In comparison with earlier procedures giving recoveries of 0.3 mg (Kuznetsov et al., 1981) or 1 mg (Vallee, 1982) of bulk MAP1 per kilogram of brain tissue, our procedure gave yields of about 1–2 orders of magnitude greater (50 mg/kg) for a single MAP1 species.

Purified MAP1A binds in a concentration-dependent manner both to polymerized and to unpolymerized tubulin, and the estimated stoichiometry of MAP1A/tubulin dimers in assembled microtubules is 1:(13–15). For MAP2/tubulin dimers, the calculated stoichiometry of 1:(8–9) is in good agreement with that reported earlier (Burns & Islam, 1984; Wallis et al., 1993). In reconstitution experiments, MAP1A efficiently promotes both nucleation and elongation phases of microtubule assembly and, like MAP2, lowers the critical concentration for tubulin polymerization. However, both the association and dissociation rate constants for MAP1A are 2–3-fold higher compared with MAP2. At high GTP concentrations, MAP1A promotes the incorporation of both oligomers and dimers into the growing microtubule, and the incorporation rate of the oligomer is also higher for MAP1A when compared with MAP2 (24×10^{-3} versus 10×10^{-3} s^{-1}).

There is therefore a general similarity in the mechanism by which MAP1A and MAP2 promote tubulin polymerization. However, MAP1A microtubules are more dynamic compared with MAP2 microtubules, and the rate constants may reflect differences in the putative MAP1A and MAP2 microtubule binding motifs (Langkopf et al., 1993). Alternatively, MAP1A and MAP2 may promote assembly by a similar mechanism but by binding to different sites on the tubulin molecule, and in this context, it is important to note that (a) there is a much greater sequence similarity in the putative microtubule binding motifs of MAP1A and MAP1B proteins but there is a striking difference in their relative affinities in terms of binding to microtubules; (b) MAP1A and MAP2 have been colocalized on the same microtubules (Shiomura & Hirokawa, 1987) but peptides corresponding to the microtubule binding motif of MAP1B have been shown to compete for MAP2 binding to microtubules; (c) in our preparations twice-cycled microtubule protein contains stoichiometric amounts of MAP1A and MAP2, suggesting that the two proteins do not compete for microtubule binding; (d) there is increasing evidence that MAPs contain more than one tubulin binding site (Chen et al., 1992); and (e) a novel acidic microtubule binding domain has recently been identified in the MAP1A molecule (Cravchik et al., 1994). The availability of purified native MAP1A, and more recent attempts using recombinant techniques, may help answer some of the questions as regards the binding motifs.

The much more widespread distribution of MAP1A, present in axons, dendrites, glial cells, interphase, and mitotic microtubules, may imply a more general function with microtubules compared with the essentially dendritic MAP2. We have recently demonstrated that MAP1A can also bind to actin and cross-link actin filaments (Pedrotti et al., 1994b), suggesting yet another property in common with MAP2. The similarities and differences in MAP1A and MAP2 interaction with cytoskeletal components will be useful in understanding the organizational role of these proteins in the cytomatrix.

ACKNOWLEDGMENT

We thank Dr. Rosamund Williams (Lepetit Research Center) for critically reading the manuscript and for helpful suggestions and Dr. M. Suffness (NIH) for the generous gift of taxol.

REFERENCES

Amos, L. (1977) *J. Cell Biol. 72*, 642–654.

Bloom, G. S., Luca, F. C., & Vallee, R. B. (1984a) *J. Cell Biol. 98*, 320–330.

Bloom, G. S., Schoenfeld, T. A., & Vallee, R. B. (1984b) *J. Cell Biol. 98*, 331–340.

Bloom, G. S., Luca, F. C., & Vallee, R. B. (1985) *Proc. Natl. Acad. Sci. U.S.A. 82*, 5404–5408.

Burns, R. G. (1991) *Biochem. J. 277*, 231–238.

Burns, R. G., & Islam, K. (1984) *Eur. J. Biochem. 141*, 599–608.

Burns, R. G., & Islam, K. (1986) *Ann. N.Y. Acad. Sci. 466*, 340–356.

Cambray-Deakin, M. A., Norman, K. M., & Burgoyne, R. D. (1987) *Dev. Brain Res. 34*, 1–7.
Chen, J., Kanai, Y., Cowan, N. J., & Hirokawa, N. (1992) *Nature (London) 360*, 674–677.
Cleveland, D. W., Hwo, S.-Y., & Kirschner, M. W. (1977) *J. Mol. Biol. 116*, 227–247.
Cravchik, A., Reddy, D., & Matus, A. (1994) *J. Cell Sci. 107*, 661–672.
Farrell, K., Jordan, M. A., Miller, H. P., & Wilson, L. (1987) *J. Cell Biol. 104*, 1035–1046.
Hasegawa, M., Arai, T., & Ihara, Y. (1990) *Neuron 4*, 909–918.
Herzog, W., & Weber, K. (1978) *Eur. J. Biochem. 92*, 1–8.
Horio, T., & Hotani, H. (1986) *Nature (London) 135*, 605–607.
Islam, K., & Burns, R. G. (1981) *FEBS Lett. 123*, 181–185.
Islam, K., & Burns, R. G. (1984) *FEBS Lett. 178*, 264–270.
Islam, K., & Burns, R. G. (1986) *Ann. N.Y. Acad. Sci. 466*, 639–641.
Johnson, K. A., & Borisy, G. G. (1977) *J. Mol. Biol. 117*, 1–31.
Kuznetsov, S. A., Rodionov, V. I., Gelfand, V. I., & Rosenblat, V. A. (1981) *FEBS Lett. 135*, 237–240.
Kuznetsov, S. A., Rodionov, V. I., Nadezhina, E. S., Murphy, D. B., & Gelfand, V. I. (1986) *J. Cell. Biol. 102*, 1060–1066.
Langkopf, A., Hammarback, J. A., Reinhold, M., Vallee, R. B., & Garner, C. C. (1992) *J. Biol. Chem. 267*, 16561–16566.
Letterier, J.-F., Liem, R. K. H., & Shelanski, M. L. (1982) *J. Cell Biol. 95*, 982–986.
Lewis, S. A., Sherline, P., & Cowan, N. J. (1988) *Science 242*, 936–939.
Mandelkow, E. M., & Mandelkow, E. (1993) *Trends Biochem. Sci. 18*, 480–483.
Matus, A. (1988) *Annu. Rev. Neurosci. 11*, 29–44.
Matus, A. (1990) *J. Physiol. (Paris) 84*, 131–137.
Noble, M., Lewis, S. A., & Cowan, N. J. (1989) *J. Cell Biol. 109*, 3367–3376.
Olmsted, J. B. (1986) *Annu. Rev. Cell Biol. 2*, 421–457.
Oosawa, F., & Kasai, M. (1962) *J. Mol. Biol. 4*, 10–21.
Papasozomenos, S. C., & Binder, L. I. (1987) *Cell Motil. Cytoskel. 8*, 210–216.
Paschal, B. M., & Vallee, R. B. (1987) *Nature (London) 330*, 181–183.
Pedrotti, B., Soffientini, A., & Islam, K. (1993) *Cell Motil. Cytoskel. 25*, 234–242.
Pedrotti, B., Colombo, R., & Islam, K. (1994a) *Biochemistry 33*, 8798–8806.
Pedrotti, B., Colombo, R., & Islam, K. (1994b) *Cell Motil. Cytoskel.* (in press).
Sattilaro, R. F. (1986) *Biochemistry 25*, 2003–2009.
Schoenfeld, T. A., McKerracher, L., Obar, R., & Vallee, R. B. (1989) *J. Neurosci. 9*, 1712–1730.
Shiomura, Y., & Hirokawa, N. (1987) *J. Cell Biol. 104*, 1575–1578.
Suprenant, K., & Dentler, W. (1982) *J. Cell Biol. 93*, 164–174.
Towbin, H., & Gordon, J. (1984) *J. Immunol. Methods 72*, 313–340.
Tucker, R. P. (1990) *Brain Res. Rev. 15*, 101–120.
Vallee, R. B. (1982), *J. Cell Biol. 92*, 435–442.
Vallee, R. B. (1985) *Biochim. Biophys. Res. Commun. 133*, 128–133.
Vallee, R. B., & Davis, S. E. (1983) *Proc. Natl. Acad. Sci. U.S.A. 80*, 1342–1346.
Vera, J. C., Rivas, C. I., & Maccioni, R. B. (1988) *FEBS Lett. 232*, 159–162.
Wallis, K. T., Azhar, S., Rho, M. B., Lewis, S. A., Cowan, N. J., & Murphy, D. B. (1993) *J. Biol. Chem. 268*, 15158–15167.
Wilson, L., & Farrell, K. (1986) *Ann. N.Y. Acad. Sci. 466*, 690–708.
Wiche, G. (1989) *Biochem. J. 259*, 1–12.